Proceedings of the 29th Annual International
Conference of the IEEE EMBS
Cité Internationale, Lyon, France
August 23-26, 2007.

Hand Pose Estimation Using EMG Signals

Masairo Yoshikawa, Member, IEEE, Masahiko Mikawa, and Kazuyo Tanaka, Member, IEEE

Abstract— **In this paper, we report a hand pose estimation using electromyogram (EMG) signals consisting of two methods. One is a method of hand motion classification with a support vector machine (SVM). The other is a method of operator's joint angle estimation based on EMG-Joint angle models, which express the linear relationships between the EMG signals and joint angles. By incorporating the motion classification and joint angle estimation, it is not discrete but continuous hand pose estimation is achieved. To examine the effectiveness of our method, we performed experiments in which seven hand motions are estimated by our method with eight subjects. Experimental results show that motion classification was performed with high accuracy and that three joint angles were estimated well for subjects experienced in our methodology.**

I. INTRODUCTION

Electromyogram (EMG) signals, which can be measured on skin surface with noninvasive electrodes, contain information for motions to be performed, such as which muscles contract, and their intensity. Deriving this information from the EMG signals, researchers have attempted to achieve a natural and intuitive human interface for controlling a robotic hand. Particularly, many applications to prosthetic hands to substitute amputee's lost hand functions have been studied. In these studies, to estimate hand motions intended by an operator using EMG patterns, various methods based on pattern classification approaches, such as artificial neural networks [1][2], fuzzy logic [3], Gaussian mixture model classifiers [4], and self-organized maps[5], have been proposed.

In this paper, we report a hand pose estimation using EMG signals consisting of two methods. One is a method of hand motion classification with a support vector machine (SVM). Although SVMs have been shown to be effective in a wide range of classification problems[6], there has been little research on the application of SVMs to hand motion classification using EMG signals. The SVMs equip superior ability to generalize and to classify linearly-inseparable patterns with small computational complexity, and their hyperparameters used in training are easily determined. Therefore, the SVMs can be an effective classifier in our purpose. As for feature extractions, cepstrum coefficients are used as frequency-domain features in combination with the time-domain features. Although the cepstrum coefficients have been used as effective features in speech recognition, it is not examined whether the cepstrum coefficients are effective features in EMG pattern classification. The other is a method of subject's joint angle estimation based on EMG-Joint angle models, which express the relationships between the EMG signals and joint angles. By incorporating the motion classification and joint estimation, it is not discrete but continuous hand pose estimation can be achieved.

To examine the effectiveness of our method, we performed experiments in which seven hand motions performed by subjects are estimated by our method.

All authors are with Graduate School of Library, Information and Media Studies, University of Tsukuba, 1-2 Kasuga, Tsukuba, Ibaraki, 305-8550 Japan (yosikawa@slis.tsukuba.ac.jp)

II. METHOD

Figure 1 shows a schematic diagram of hand pose estimation. First, EMG signals and integrated EMG (IEMG) signals are measured using surface electrodes placed on a subject's forearm. Next, features are extracted from the EMG and IEMG signals for motion classification. A feature vector consists of both time and frequency domain features. Then, the feature vector is classified based on decision functions obtained by the SVM. As a result, an subject's hand motion is decided. Finally, a joint angle corresponding to a decided hand motion is estimated based on an EMG-Joint angle model.

A. Signal Measurement

The EMG signals are measured with bipolar surface electrodes. These signals are amplified and converted into IEMG signals by applying full-wave rectification and smoothing (cutoff frequency 2.4 Hz) using an EMG measurement instrument. The EMG and IEMG signals are sampled at 2 KHz using a 16-bit A/D converter.

B. Feature Extraction

Features are extracted from the EMG and IEMG signals in the 64-ms frame, which is shifted for 16 ms. These processes provide the frame length necessary for feature extraction, and achieve a 16-ms estimation period.

The three types of features are extracted from each frame: averaged IEMG (AIEMG), cepstrum coefficients (CC), and delta cepstrum coefficients (DCC).

The AIEMG features are averaged IEMG signals in each frame, which express the magnitude of the EMG signals. In conventional researches, these features have been combined with other features.

The CC features are cepstrum coefficients, computed by the inverse fourier transform of the logarithmic power spectrum of the EMG signals. When the n^{th} sampled EMG signals measured with the l^{th} electrode at the p^{th} frame is defined as $IEMG_l(n)$ $(n = 0, \cdots, N-1;\ l = 1, \cdots, L)$, the cepstrum coefficients $CC_l^n(p)$ are calculated as follows:

$$CC_l^n(p) = \frac{1}{N} \sum_{k=0}^{N-1} \log |\mathcal{F}[EMG_l(n)]| e^{j2\pi kn/N}, \quad (1)$$

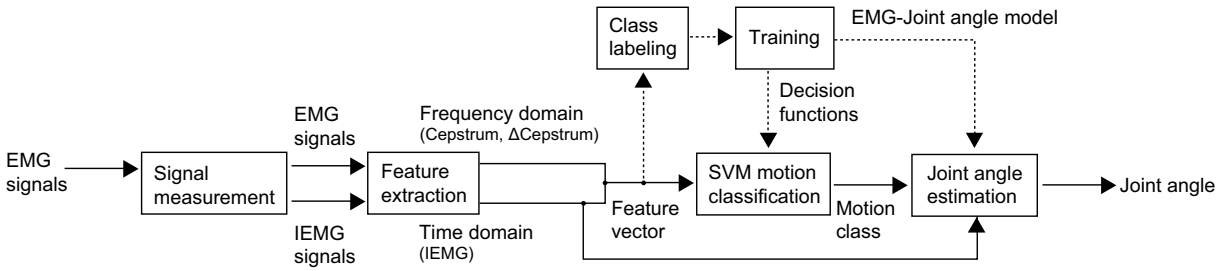

Fig. 1. Schematic diagram of hand pose estimation

where $\mathcal{F}[EMG_l(n)]$ denotes the fourier transform of $EMG_l(n)$. The low-order cepstrum coefficients contain spectrum envelope information, which is often used in speech recognition to achieve robust classification with small dimensional feature vectors. We used the cepstrum coefficients $CC_l^n(p)$ $(n = 0, 1, \cdots, W-1)$ as the CC features, where W is a CC feature parameter.

The CC features are static features extracted from the EMG signals in the frame. However, spectrum features change continuously with time. Thus, by adding dynamic features across frames, classification performance can be improved. We use the DCC feature as a dynamic feature. The DCC features $DCC_l^h(p)$ $(h = 0, \cdots, W-1)$ are calculated as follows:

$$DCC_l^h(p) = CC_l^h(p) - CC_l^h(p - Z) \tag{2}$$

where Z is a DCC feature parameter.

In this study, $W = 3, Z = 8$, which gave the best classification performance in preparatory experiments, were used in the following experiments. Four electrodes ($L = 4$) were placed on a subject's forearm surface over the flexor carpi ulnaris, extensor carpi radialis, flexor digitorum profundus, and extensor digitorum. Provided that all features are used, 1-dimensional AIEMG features, 3-dimensional CC features, and 3-dimensional DCC features are extracted for each electrode, resulting in a 28-dimensional feature vector.

C. Hand Motion Classification Using SVM

In this section, we describe the motion classification with the SVM. The decision function classifying the unknown feature vector $\boldsymbol{x}$ in a two-class problem is expressed as

$$f(\boldsymbol{x}) = \text{sign}(\sum_{i=1}^{D} \lambda_i y_i K(\boldsymbol{x}_i, \boldsymbol{x}) + b), \tag{3}$$

where y_i is a class label corresponding to the i^{th} training sample $\boldsymbol{x}_i$, D is the number of training samples, λ_i is a lagrange multiplier, and b is a bias. A radial basis function (RBF) kernel is used as the kernel function K in our method,

$$K(\boldsymbol{x}_i, \boldsymbol{x}) = \exp\left(-\gamma ||\boldsymbol{x}_i - \boldsymbol{x}||^2\right), \tag{4}$$

where γ is a kernel parameter. This RBF kernel non-linearly maps samples into a higher dimensional space and allows linear classification in this space. The decision function in Eq. 3 can be obtained by solving the following dual optimization problem:

$$\max_{\boldsymbol{\lambda}} \quad \sum_{i=1}^{D} \lambda_i - \frac{1}{2} \sum_{i,j=1}^{D} \lambda_i \lambda_j y_i y_j K(\boldsymbol{x}_i, \boldsymbol{x}) \tag{5}$$

$$\text{subject to} \quad \sum_{i=1}^{D} \lambda_i y_i = 0, \ 0 \le \lambda_i \le C \tag{6}$$

where $\boldsymbol{x}_i$ is a support vector corresponding to nonzero λ_i, and C is the regularization constant that decides the degree of classification errors. Because only the kernel parameter γ and the regularization parameter C have to be optimized, these parameters can be obtained by a grid search.

In our method, seven hand motion classes shown in Fig. 2 were treated: neutral, flexion, extension, grasp, open, pronation, and supination. To solve the multi-class classification problem, we use a one-against-one algorithm proposed by Knerr et. al.[7]

Sudden misclassification, caused by noises and variations in the EMG signals, can occur when the subject performs the same motion. To improve this kind of misclassification, we use a majority vote: the hand motion class is decided by voting for the classification results in the current frame and previous five frames.

D. Joint Angle Estimation

After the hand motion performed by the subject has been determined, the joint angle corresponding to the motion is estimated by the EMG-Joint angle model. The estimated joint angles θ_{ca} $(a = 1, \cdots, 3)$ in motion c $(c = 1, \cdots, 6)$ are shown in Fig. 2. The average of AIEMG features of the L electrodes in the p^{th} frame is calculated as follows:

$$E(p) = \frac{1}{L} \sum_{l=1}^{L} AIEMG_l(p). \tag{7}$$

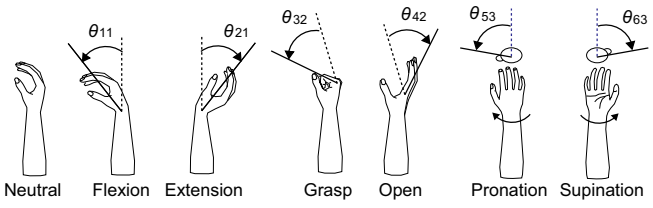

Fig. 2. Seven hand motions and estimated joint angles

Because we suppose that the relationships between the EMG signals and joint angles can be approximated by linear models in preparatory experiments, using $E(p)$, the EMG-Joint angle model can be expressed as

$$\hat{\theta}_{ca}(p) = \frac{E(p) - E_{ca}^{min}}{E_{ca}^{max} - E_{ca}^{min}} \theta_{ca}^{max}, \tag{8}$$

where θ_{ca}^{max} is the maximal angle in the movable range of the joint angle a, whose sign is dependent on the motion c. E_{ca}^{max} and E_{ca}^{max} are the maximal and minimal values of $E(p)$ when the subject varies joint angle a in motion c, respectively. These values are preliminarily obtained from the training data.

III. Experiment

To evaluate our method, we performed experiments with eight healthy subjects (four male and four female, aged between 20 and 36 years). Subjects A, B, and E were accustomed to the measurement of the EMG signals, while the other subjects were experiencing this methodology for the first time. In one experimental trial, the subjects were required to perform seven hand motions, as shown in Fig. 2, sequentially for 60 s. A three-dimensional computer graphics (3DCG) robot hand on a computer display shown in Fig. 3 directed the subjects motions to be performed. Hand motions were performed in the order of flexion, extension, grasp, open, pronation, and supination. Each motion was performed five times to the maximal angle in the movable range, and returned to the neutral in about one second. EMG signal data from 22 trials were recorded with an interval of about 20 s. The first trial data were used as training data, and the other 21 trial data were used as test data. To prepare the training and test data, the feature vectors were labeled based on zero crossings of the EMG signals. To monitor the subject's joint angles, the wrist and finger MP joint angles were measured with shape sensors (Shapesensor, Measurand Inc.), while the pronation/supination angle was measured with a three-axis acceleration sensor (HAAM-313B, Hokuriku Electric Industry Co. Ltd.). We used the LIBSVM library [8] for SVM training and motion classification.

A. Effect of Feature Selection and SVM Parameter Optimization

To examine the effect of feature selection, we compare the classification rate for three types of feature vectors: AIEMG (4-dimensional), AIEMG+CC (16-dimensional), and AIEMG+CC+DCC (28-dimensional). The left three bars in Fig. 4 shows the classification rates, averaged across eight subjects, for three types of feature vectors. The SVM parameters were $\gamma = 0.5$ and $C = 32$. From this figure, the AIEMG+CC feature vector shows much better classification rate than the AIEMG feature vector by 5.4% (one-side t-test: $p < 0.01$). When the DCC features were added to the AIEMG+CC feature vector, accuracy was improved by 0.7% (one-side t-test: $p < 0.05$). Moreover, the right bar in Fig. 4 shows the classification rate when training was performed using optimal SVM parameters. The optimal SVM parameters, γ and C, were determined by a grid search using the training data for each subject. The search ranges of γ and C were $\gamma = \{2^{-5}, 2^{-4}, \cdots 2^{0}\}$ and $C = \{2^{1}, 2^{2}, \cdots, 2^{8}\}$, respectively. In each grid point, 5-fold cross validation was performed, and the combination of γ and C that provided the best classification accuracy was searched. Consequently, the classification rate was improved by 6.7% compared to the AIEMG feature vector. In the following results, the AIEMG+CC+DCC feature vectors and optimized SVM parameters were used.

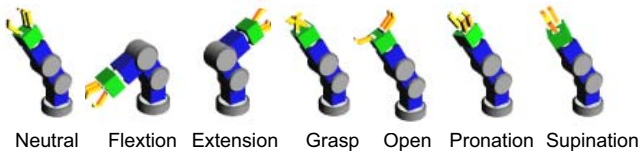

Fig. 3. 3DCG robothand directing subjects motions to be performed

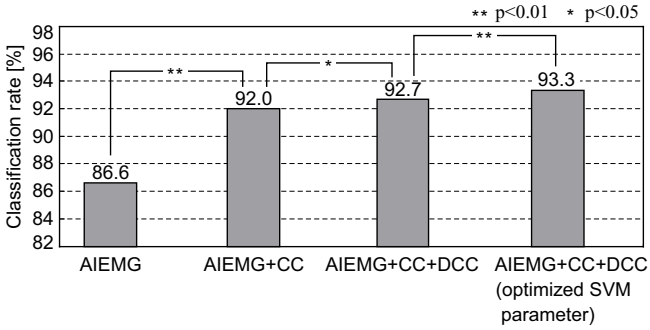

Fig. 4. Effect of feature selection and SVM parameter optimization

TABLE I
Classification results for each motion

Subject	0	1	2	3	4	5	6
A	93.7	97.1	97.1	93.8	95.6	95.4	89.7
B	95.5	93.1	94.2	94.6	94.5	89.5	91.5
C	96.3	91.5	90.7	89.0	89.3	79.1	83.1
D	98.9	83.0	86.9	80.9	88.6	80.9	81.4
E	94.2	95.2	93.3	93.2	92.2	86.5	91.8
F	95.3	96.6	92.3	79.5	94.1	84.8	90.5
G	95.9	94.2	82.1	84.8	91.1	81.6	56.5
H	95.7	94.9	92.3	81.0	86.0	92.5	72.6
Mean	95.7	93.3	91.3	87.2	91.6	85.8	83.7

0:Neutral 1:Flexion 2:Extension 3:Grasp 4:Open 5:Pronation 6:Supination

B. Motion Classification Results

Table I shows the classification rate for each motion. From this table, the high classification accuracy was observed for Subjects A, B, and E across all types of motions. On the other hand, there were a few motions in which the classification rates were less than 85% for the other subjects. Subjects A, B, and E were experienced in controlling the EMG signals, and their electrode positions were identified to classify the EMG patterns. Acquiring a same experience, the other subjects can show better classification performance.

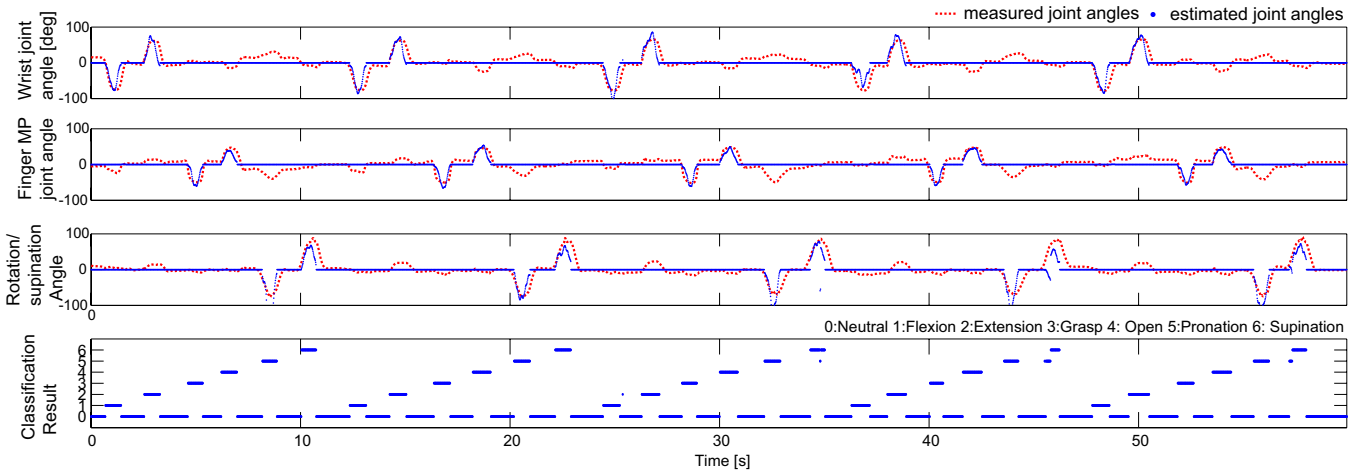

Fig. 5. An example of joint angle estimation for Subject A

The classification rates of pronation and supination are lower than that of the other motions because we could not measure muscles involved in these motions directly.

C. Joint Angle Estimataion

Fig. 5 shows joint angle estimation result in the last trial for Subject A. The subject performed seven hand motions in the order of flexion, extension, grasp, open, pronation, and supination. The upper three graphs show the estimation results of the subject's wrist joint angles, finger MP joint angles, and pronation/supination angles. The dashed line and dots denote the measured and estimated joint angles, respectively. The lower graph shows the motion classification results. These graphs show that hand motion classification was performed with high accuracy and that the three joint angles were estimated well and without delay. However some classification errors were observed during the supination.

D. Robustness to Variations of EMG Signals

Due to fatigue, sweating, and electrode shifts, the features of the EMG signals change with time. Figure 6 shows the variations of classification rate, averaged across eight subjects, with trial number. The result shows that the classification rates are more than 92% across 21 trials. So, it is suggested that the generalization ability of SVM works well in EMG pattern classification.

IV. Conclusions

In this paper, we reported a hand pose estimation using electromyogram (EMG) signals consisting of two methods: hand motion classification with a SVM and joint angle estimation based on EMG-Joint angle models. To examine the effectiveness of our method, we performed experiments in which seven hand motions are estimated by our method with eight subjects. Experimental results show that motion classification was performed with high accuracy and that three joint angles were estimated well for subjects experienced in our methodology.

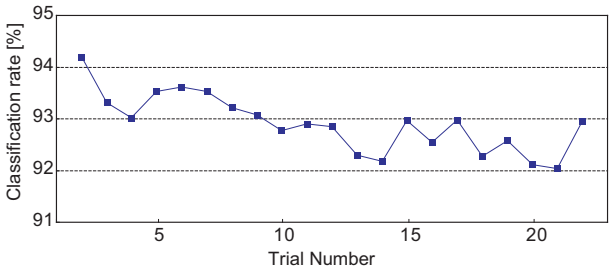

Fig. 6. Variations of classification rate, averaged across eight subjects, with trial number

V. Acknowledgments

This work was supported by a Grant-in-Aid for Scientific Research (19500377).

References

[1] M. F. Kelly, P. A. Parker, and R. N. Scott, "The application of neural networks to myoelectric signal analysis: A preliminary study," *IEEE Trans. Biomed. Eng.*, vol. 37, no. 3, pp. 221–230, 1990.

[2] O. Fukuda, T. Tsuji, M. Kaneko, and A. Otsuka, "A human-assisting manipulator teleoperated by EMG signals and arm motions," *IEEE Trans. Robot. Automat.*, vol. 19, no. 2, pp. 210–222, 2003.

[3] A. B. Aiiboye and R. F. Weir, "A heuristic fuzzy logic approach to EMG pattern recognition for multifunctional prosthesis control," *IEEE Trans. Neural Syst. Rehab. Eng.*, vol. 13, no. 3, pp. 280–291, 2005.

[4] Y. Huang, K. B. Englehart, B. Hudgins, and A. D. C. Chan, "A gaussian mixture model based classification scheme for myoelectric control of powered upper limb prostheses," *IEEE Trans. Biomed. Eng.*, vol. 52, no. 11, pp. 1801–1811, 2005.

[5] J. U. Chu, I. Moon, and M. S. Mun, "A real-time EMG pattern recognition system based on linear-nonlinear feature projection for a multifunction myoelectric hand," *IEEE Trans. Biomed. Eng.*, vol. 53, no. 11, pp. 2232–2239, 2006.

[6] S. W. Lee and A. Verri, Eds., *Pattern Recognition with Support Vector Machines, First International Workshop, SVM 2002, Proceedings*. Springer, 2002.

[7] S. Knerr, L. Personnaz, and G. Dreyfus, "Single-layer learning revisited: a stepwise procedure for building and training a neural network," in *Neurocomputing: Algorithms, Architectures and Applications*, F. Fogelman and J. Herault, Eds. Springer-Verlag, 1990.

[8] C. C. Chang and C. J. Lin, *LIBSVM: a Library for Support Vector Machines*, 2001, software available at http://www.csie.ntu.edu.tw/ cjlin/libsvm.